Journal of Systems Engineering and Electronics
Vol. 28, No. 5, October 2017, pp.934 – 945

Multi-objective evolutionary optimization for geostationary orbit satellite mission planning

Jiting Li*, Sheng Zhang, Xiaolu Liu, and Renjie He

College of Information System and Management, National University of Defense Technology, Changsha 410073, China

Abstract: In the past few decades, applications of geostationary orbit (GEO) satellites have attracted increasing attention, and with the development of optical technologies, GEO optical satellites have become popular worldwide. This paper proposes a general working pattern for a GEO optical satellite, as well as a target observation mission planning model. After analyzing the requirements of users and satellite control agencies, two objectives are simultaneously considered: maximization of total profit and minimization of satellite attitude maneuver angle. An NSGA-II based multi-objective optimization algorithm is proposed, which contains some heuristic principles in the initialization phase and mutation operator, and is embedded with a traveling salesman problem (TSP) optimization. The validity and performance of the proposed method are verified by extensive numerical simulations that include several types of point target distributions.

Keywords: geostationary orbit (GEO) satellitemission planning, multi-objective optimization, evolutionary genetic.

DOI: 10.21629/JSEE.2017.05.11

1. Introduction

An imaging satellite is an earth observation satellite that uses a satellite borne remote sensor to acquire ground image information from space [1]. Geostationary orbit (GEO) satellites, also known as high orbit satellites, are important imaging satellites that are used worldwide and play an important role in various fields such as communication, land surveying, situational awareness, weather forecasting, and emergency response [2]. Among different kinds of GEO satellites, GEO high resolution optical satellite has developed rapidly in recent years.

Given the rapid developments in optical camera technology, some countries have begun to apply high resolution optical cameras in geosynchronous orbit; such an application utilizes the advantages of high orbit residence time and meets the needs of certain military and civilian applications. Information on some typical GEO high resolution (HR) optical imaging satellites in different countries are shown in Table 1.

Table 1 GEO high resolution optical imaging satellites in different countries

Country	Name of satellite	Spatial resolution/m
India	GEO-HR IMAGER	60
France	GEO-20m-OIS [3]	20
France	GEO-AFRICA [4]	25
ESA	GEO-OCULUS [5]	10
China	GF-4[6]	50

The GEO-Africa satellite of the European Astrium company has attracted significant attention; the satellite is proposed for low latitudes in Africa and is to be used for the observation of agriculture, land, coasts, and other natural resources. The satellite launched by India can cover India's territory every half hour, and is mainly used for monitoring crops, surveying resources, and monitoring disasters. In China, GEO high resolution optical satellites have been developed with a spatial resolution of 50 m that are used for investigating resources and monitoring disasters.

GEO satellite mission planning is a typical example of a satellite mission planning problem. Satellite mission planning is the process of rational allocation of satellite resources in order to improve the observation profits [7]. The imaging satellite mission planning problem is related to computer science, operations research, and artificial intelligence. For the mission planning of medium and low orbit satellites, researchers from various fields have developed modeling schemes from different perspectives [8 – 12]. And in recent years, the system design and mission planning of autonomous satellite becomes a hot issue in this area [13 – 15].

Currently, GEO satellite planning is primarily about trusting the station to maintain maneuver planning [16], satellite refueling planning [17], and radio planning in GEO satellite networks [18]. However, studies on GEO satellite observation are limited, and existing literature

Manuscript received May 08, 2017.
*Corresponding author.
This work was supported by the National Natural Science Foundation of China (71501180; 61473301).

mainly focus on applications of GEO satellite observation towards earth and introductions to the function of GEO satellites. Akimoto et al. [19] introduced the application of air pollution observation via GEO satellites. Finke et al. [20] studied how to detect and locate lighting events by GEO satellite observations. Chen [21] considered the cloud effect on lighting detection by GEO satellites. Orphal et al. [22] presented the geostationary Fourier imaging spectrometer (GeoFIS) in order to improve the predictive capability of tropospheric chemistry models. Reference [5] provided a brief introduction to the applications of GeoOculus and its high resolution camera.

The orbital height of GEO satellites is 36 000 km, and with its large width and orbital advantages, the satellite can cover a wide area. The satellite has a dedicated ground station that can continuously track targets. All these features make its scheduling different from other types of satellites. Currently, GEO satellites are widely used for large-scale area scanning. However, during daily use of GEO satellites, we often encounter users that ask to shoot some targets directly in a large area. This type of functionality would require a customized approach and is a new problem for us. We define this type of problem as a GEO optical satellite earth observation task planning problem. To the best of our knowledge, there is no literature that builds a mission planning model of GEO satellite observation on earth; thus, this is the main motivation of this research. Based on the requirements of users and further development of GEO satellites, this paper builds a multi-objective model for mission planning of GEO satellite observation on earth.

The contributions of this paper include: (i) proposing a general working pattern for a GEO optical satellite, (ii) building a multi-objective model for the problem proposed in this paper, and (iii) proposing an NSGA-II based method to solve the model.

The rest of this paper is organized as follows. Section 2 presents a working pattern for GEO optical satellites and a description of the multi-objective scheduling problem. A mathematical model is also introduced in it. Section 3 introduces the improved NSGA-II algorithm used in this paper. Numerical simulation results are provided in Section 4, which include situations with different scales and distributions of observation targets and comparisons. The conclusion is provided in Section 5.

2. Problem description and mathematical model

A GEO satellite can remain stationary in the space above a certain latitude of the earth and obtain images using the affixed camera. One special characteristic of GEO satellites is the time window of observation. The orbital period of a GEO satellite is 24 hours, and a daily working process can be divided into two stages: daytime stage and night stage. A working flow chart of a GEO optical satellite is shown in Fig. 1.

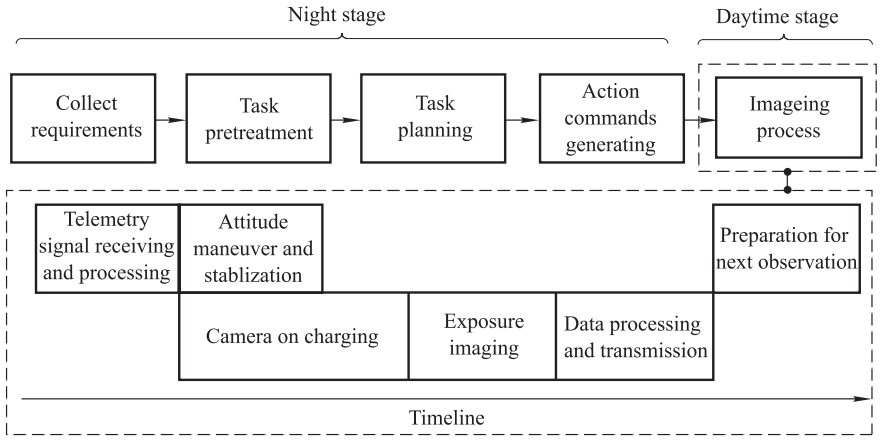

Fig. 1 Working flow chart of a GEO optical satellite

In Fig. 1, during the daytime stage, the visible region of the GEO satellite is under the sun, and thus the visible time window is very long. In the time window, every imaging process of a GEO satellite includes telemetry signal receiving and processing, attitude maneuver and stabilization processing, and so on. In the night stage, most, or all, of the area within the visible range of the satellite is not exposed to sunlight and cannot be imaged. In this stage, the ground transportation control department collects task requirements and arranges imaging tasks for the next daytime stage and sends action commands to the satellite.

In the working flow chart, task planning for the GEO satellite is the most important. The observation task of a GEO satellite can be summarized into three categories: scan task, periodic task, and gaze task. This paper focuses mainly on the task planning part and the scan task is the

main concerning mission. When performing a scan mission, the satellite only observes the target once. Low orbit satellites primarily use stripes to observe targets, but a GEO satellite uses single views to observe targets. A single view is one satellite camera shooting area, which is square and has a standard size. However, during the observation process, due to the different latitudes and longitudes of targets, a GEO satellite will need to adjust its attitude, so the single view will be deformed, becoming larger than the standard size. Depending on size, observation targets can be grouped into two types: point targets and regional targets. The main content of this paper discusses the observation of point targets. A simplified map of a GEO satellite observing point targets is shown in Fig. 2.

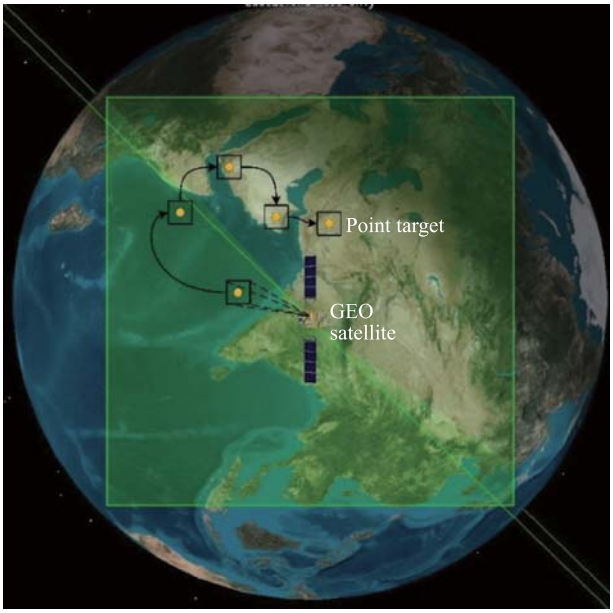

Fig. 2 Simplified map of a GEO satellite observing point targets

In Fig. 2, the small grid represents a single view field of the camera and the larger grid is the biggest area covered by the GEO satellite. Solid dots represent fixed point targets, which have various types of distributions.

In future applications of GEO satellites, a large number of civilian users will be served. When faced with very important users, their needs should be satisfied, but for general users with various sized point target observation needs, satellite control agency should make balanced decisions. In order to complete as many of the scheduled tasks as possible, the time of each imaging mission must be limited, and an important related factor is the number of single scene photos. Further, by analyzing the needs of users and of the satellite control agency, we find three main indicators of concern: total profit, time cost, and energy consumption. And the satellite's attitude maneuver angle is closely related to the two latter indicators. Thus the problem we solve in this paper can be described as under the limited number of single view photos, two objectives should be considered on the balance of users' needs and satellite's consumption: total profit maximization and minimization of the satellite's attitude adjustment angle. The conflicts between these two goals is illustrated in Fig. 3.

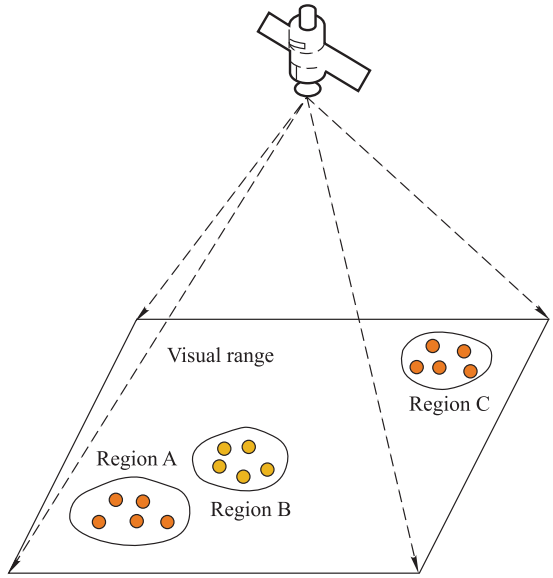

Fig. 3 Confliction of two objectives

As shown in Fig. 3, the profit of point targets in region A is high and the profit of point targets in region B is small. Although the profit for region C is slightly higher than that for region B, it is far away from regions A and B. If the satellite takes images of region C, the adjustment angle will be larger, which will influence energy consumption and the time required. Therefore, when faced with such conflicts, it is necessary to develop appropriate planning.

In order to optimize the angle adjustment sequence, the observation order for a series of photographs can be modeled as a traveling salesman problem (TSP), where the goal is to find the optimal angle adjustment sequence to ensure that the sum of the attitude maneuver angles is minimized.

The GEO satellite for observation in orbit is denoted as S_{GEO}, its orbital height is denoted as h. For simplicity, we regard its single view and visual range both as square. The length of the side of single view is r, and the length of the side of visual range is L. The set of point targets to be observed is denoted as $T = \{t_1, \ldots, t_m\}$, where M is the target number. Each target t_m has coordinates information which is represented as (x_{t_m}, y_{t_m}), $m = 1, \ldots, M$. If the target t_m is observed, its associated profit is p_m. For the attitude maneuver of satellite S_{GEO}, the adjustment angle of it along horizontal and vertical directions, named as

roll angle and pitch angel are α and β, respectively. The maximum adjustment scopes of them are $\alpha_{\max}$ and $\beta_{\max}$. The number of images to be taken is represented as N. The coordinate of the central point of each image g_n is (x_{g_n}, y_{g_n}) and $n = 1, \ldots, N$. The number of point targets contained in each photo is denoted as ng_n. The visual range of GEO satellite is denoted as a square with vertexes $y_{\max}, y_{\min}, x_{\max}$ and $x_{\min}$. It is assumed that the project coordinates of the satellite are $(x_{\max} + x_{\min})/2$ and $(y_{\max} + y_{\min})/2$ and the camera is perpendicular to the ground. The decision variables of the problem consist of two components: the coordinate of the central point of each image and the observation sequence of photos.

As discussed in Section 3, for the addressed problem, we consider two objectives: maximization of revenue and minimization of total satellite attitude adjusted angles. The objectives are calculated as follows.

Objective function F_1 calculates the total profit gained during one observation mission. The profit of each point targets is a random integer, and a bigger number represents a bigger profit. As shown in Fig. 4, the coordinate of a certain single view is $[x_{g_n}, y_{g_n}]$, according to the size of single view, we can get the coordinate range of each single view, then by comparing with the coordinates of point targets, we can obtain the point targets that each single view covers.

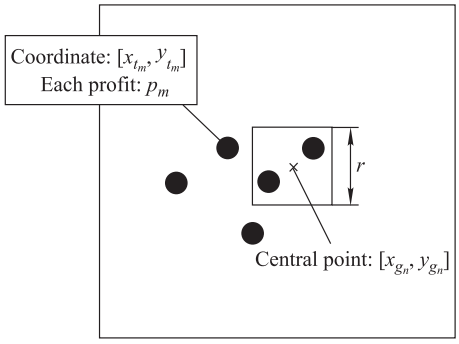

Fig. 4 Sketch map of the calculation of objective function F_1

From Fig. 4, we can get a 0-1 function, this function can show that whether targets can be included in one picture or not. And number 1 represents the point target is observed in one certain photo, and number 0 represents the point target has not been observed.

$$\mathrm{Obs}(t_m, g_n) = \begin{cases} 1, & |x_{t_m} - x_{g_n}| \leqslant \dfrac{r}{2} \cap |y_{t_m} - y_{g_n}| \leqslant \dfrac{r}{2}, \\ & 1 \leqslant m \leqslant M, 1 \leqslant n \leqslant N \\ 0, & \text{otherwise} \end{cases} \tag{1}$$

Objective function F_2 calculates the satellite attitude maneuver angle. In the calculation, for simplicity, we assume the surface of the Earth as a plane. As shown in Fig. 5, sub-satellite point [23] is the projection point of the satellite on the earth. The angle $\alpha_{i,i+1}$ and $\beta_{i,i+1}$ is the roll angle and pitch angle between photo g_i and g_{i+1}, respectively.

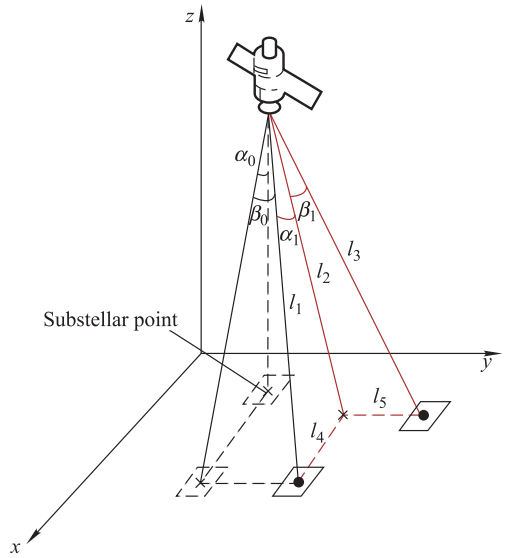

Fig. 5 Sketch map of the calculation of objective function F_2

Take Fig. 5 as an example. The Euclidean distances between the satellite and point targets are l_1, l_2, l_3. And l_4, l_5 are vertical distance and horizontal distance on the plane respectively. Then combined with the cosine formula, we can obtain the attitude angle. For example, the angle α_1 and β_1 can be calculated by formulas below:

$$\alpha_1 = \cos^{-1} \frac{l_1^2 + l_2^2 - l_4^2}{2 l_1 l_2} \tag{2}$$

$$\beta_1 = \cos^{-1} \frac{l_2^2 + l_3^2 - l_5^2}{2 l_2 l_3}. \tag{3}$$

Then, the optimization problem can be written as follows:

$$\text{obj. } \max F_1 = \sum_{i=0}^{M} \mathrm{Obs}(t_m) * p_m \tag{4}$$

$$\min F_2 = \sum_{i=0}^{n} \alpha_{i,i+1} + \beta_{i,i+1} \tag{5}$$

$$\text{s.t. } \alpha_{\max} \leqslant 8.5^\circ, \beta_{\max} \leqslant 8.5^\circ \tag{6}$$

$$x_{g_i} \neq x_{g_j} \cap y_{g_i} \neq y_{g_j}, \forall i \neq j \tag{7}$$

$$\sum_{n=1}^{N} \mathrm{Obs}(t_m, g_n) \leqslant 1, m = 1, 2, \ldots, M \tag{8}$$

$$x_{\min} \leqslant x_{t_m} \leqslant x_{\max} \tag{9}$$

$$y_{\min} \leqslant y_{t_m} \leqslant y_{\max} \tag{10}$$

$$x_{\min} \leqslant x_{g_m} \leqslant x_{\max} \tag{11}$$

$$y_{\min} \leqslant y_{g_m} \leqslant y_{\max}. \tag{12}$$

We solve the multi-objective optimization problem of GEO satellite observation problem satisfying various constraints. All of the constraints and the objectives are described in the above formulations. Constraint (6) states that the maximum capability of satellite attitude adjustment is 8.5. Constraint (7) states that every two photos cannot completely overlap with each other. In this paper, we mainly discuss scan tasks, and constraint (8) ensures that each point target is only observed once. And constraints (9)–(12) ensure that the random generation of the target coordinates and the initial population are effective.

3. Methodology

Since we simultaneously consider two objectives, similar to other combinatorial problems, a multi-objective evolutionary algorithm (MOEA) is preferable as a type of heuristic search algorithm [24,25]. A more detailed introduction to MOEAs is provided by Deb [26] and Coello et al. [27]. The addressed problem is also an NP-hard problem. We employ a classic MOEA, named NSGA-II [28], as the fundamental component of our proposed algorithm. In NSGA-II, the parent population and offspring are combined and sorted in order to generate a population for the next generation. NSGA-II ranks individuals based on two criteria. First, a non-dominated sorting mechanism is performed to classify the combined population into different groups of non-domination. Second, within a group, solutions are ranked based on the crowding distance, which ensures that diversity is maintained among the non-dominated solutions. The NSGA-II algorithm is mainly applied on continuous problems, but the proposed problem is discrete, so chromosome and genetic operators need to be modified.

3.1 Encoding and initialization

Encode is the primary and the key step to apply the genetic algorithm. And the encoding methods affect the crossover operator and the mutation operator, which determines the efficiency of genetic evolution. The most frequently used encoding methods [29] are: (i) binary code, similar to the biological chromosome structure, in which each of the individual genes is the binary number that is 0 or 1; (ii) integer coding, in which each of the individual genes is in a certain range of integers; (iii) real coding, in which each gene value is within the set of real numbers. Here, according to the characteristic of this problem, we use the matrix real coding method.

Since the problem has two types of decision variables, the chromosome consists of two parts, shown as in Fig. 6.

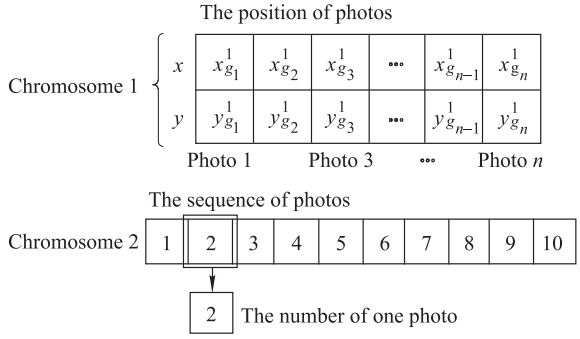

Fig. 6 Structure of chromosome

Chromosome 1 represents the position of photos, we make the coordinate of the central point of each single scene as real code. And each individual in the population is a matrix:

$$\boldsymbol{G}_k = \begin{bmatrix} x_{g_1}^k \cdots x_{g_n}^k \cdots x_{g_N}^k \\ y_{g_1}^k \cdots y_{g_n}^k \cdots y_{g_N}^k \end{bmatrix} \tag{13}$$

where $\boldsymbol{G}_k$ denotes the kth individual of the population, $x_{g_n}^k$ and $y_{g_n}^k$ are the ordinate and abscissa of the coordinates of the center point of the nth single view. Chromosome 2 represents the sequence of photos. In this paper, the sequence of photos can be regarded as a simple TSP, and in chromosome 2, each number represents one photo, and the order of numbers reflects the order of photos. By adjusting the order of photos, the satellite maneuver angles can be smaller. At the same time, optimization of the photo sequence is carried out in the Pareto frontier solution. It is impractical to optimize each feasible solution. Since the TSP is an NP-hard problem, once the number of targets or photos is too large, the embedded optimization algorithm consumes more time and slows down the speed of the NSGA-II algorithm.

In order to improve the performance of the NSGA-II algorithm, based on the daily experience of using GEO satellites, a heuristic principle is added in the initialization process of the algorithm, which is illustrated in Fig. 7.

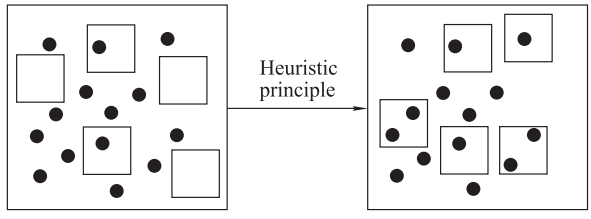

Fig. 7 Illustration of heuristic principle in initialization phase

The simple NSGA-II algorithm generates the initial population randomly, which may contain many blank photos. That hardly infects the efficiency of the evolutionary

process. The heuristic principle is that the initial position of each single scene photo must contain one point target at least. And we rename the NSGA-II algorithm with the heuristic principle as heuristic NSGA-II (HNSGA-II).

3.2 Crossover and mutation operators

The method we use to select two individuals from the parent generation is binary tournament. Then, we generate a binary string which has the same length as the parent individual randomly, in which 0 represents non-exchange and 1 represents exchange. The number of 1s is generated randomly from 1 to 3. As illustrated in Fig. 8, according to the template of the binary string, we can cross two parent individuals and obtain new offspring.

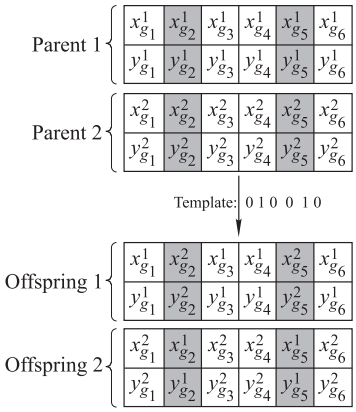

Fig. 8 Crossover operation of chromosome 1

For the sequence of photos, the crossover operation used in this paper is shown in Fig. 9. Two parent chromosome is a group, each of which repeats the following procedure: (i) generate two random integers r_1 and r_2 in the [1,10] interval, determining the two positions, crossing the intermediate data of these positions; (ii) after crossing, there are duplicate target numbers in the same chromosome, non-repetitive numbers are retained. By using partial mapping, the conflicted numbers are eliminated, that is, mapping with the corresponding relationship of the middle segment.

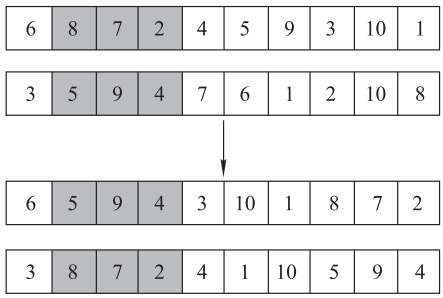

Fig. 9 Crossover operation of chromosome 2

The creation of offspring is given as follows:

Step 1 Select parent individuals $(G_i^{(1,l)}, G_i^{(2,l)})$ by binary tournament;

Step 2 Generate a random number $r \in [0, 1]$ and set the crossover possibility p_c. If $r < p_c$, go to Step 3, otherwise, this is non-exchange;

Step 3 Generate a binary string randomly and create offspring $(G_i^{(1,l+1)}, G_i^{(2,l+1)})$ using the crossover operator.

The crossover operator can yield good individual coding structure from a global perspective and is near the optimal solution. However, the algorithm can easily have a premature phenomenon.

A mutation operator can improve the local search ability of the genetic algorithm, maintain population diversity, and prevent premature convergence. We also use a heuristic principle on the mutation operator, which states that one of the central point's coordinate of the single grid can change to the coordinates of a target point with a small probability, rather than being a random movement. In the chromosome photo sequence, the mutation operation consists of randomly selecting two photos and exchanging their order.

3.3 HNSGA-II algorithm

Based on the content discussed in this paper, the basic process for the algorithm in this paper is described below and shown in Fig. 10:

Step 1 Acquire the distribution and coordinates of point targets on map and the number of sigle scene photos;

Step 2 Set the simulation parameters such as population number, maximum generation number, and crossover and mutation probabilities;

Step 3 Generate an initial population $P0$;

Step 4 Adjust the initial solution set to satisfy the constraint conditions. Evaluate objective functions, perform non-dominated sorting (i.e., sort population according to each objective function value in ascending order), and calculate crowding distance for individuals and sort according to crowding distance. Obtain the first generation $P1$. The generation count N_{gen} is equal to 1;

Step 5 Perform crossover and mutation for population $P1$, obtain the offspring generation $Q1$, adjust the solution set, and evaluate objective functions for individuals in $Q1$;

Step 6 Merge the parent population $P1$ and offspring population $Q1$, perform non-dominated sorting, calculate the crowding distance for individuals, and sort according to the crowding distance in each non-dominated layer;

Step 7 Select individuals located at the front of the set and perform embedded TSP optimization, then obtain the new parent population $P2$;

Step 8 $P1$ is equal to $P2$, increment N_{gen}, and record $P1$;

Step 9 Repeat Steps 5 to 8 until the count reaches the maximum generation number.

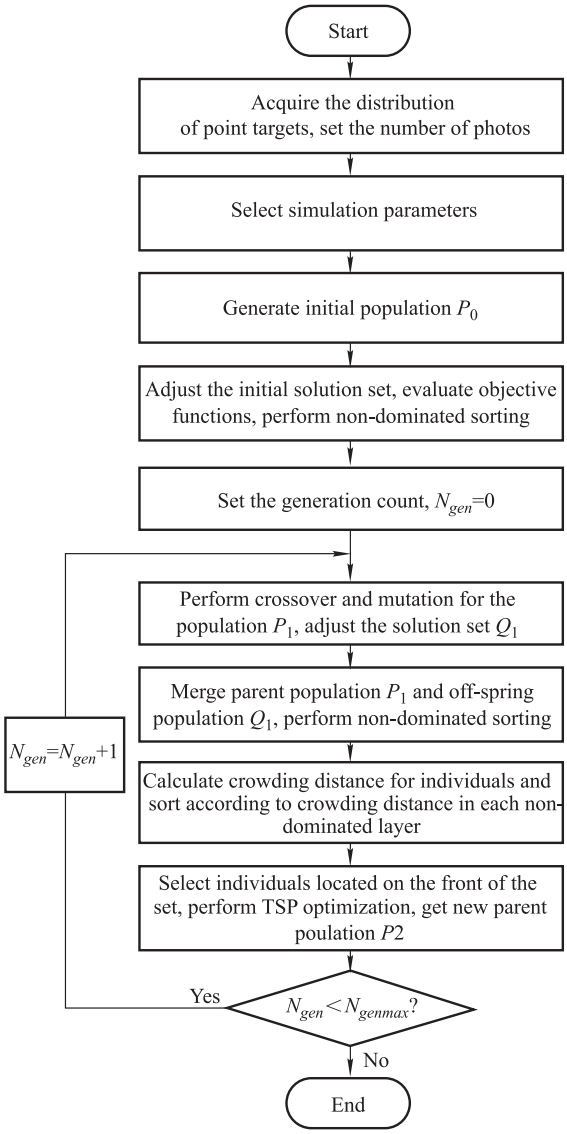

Fig. 10 Flowchart for HNSGA-II algorithm

3.4 Performance measure

In multi-objective optimization, the quality of obtained non-dominated solutions is typically measured using convergence to the Pareto front and by the distribution of solutions. Since the actual Pareto front of the proposed problem is unknown, during the evolutionary process we record a hypervolume [30] indicator, which is a comprehensive evaluation index that measures the quality of the obtained non-dominated set, and is a Pareto-compliant method.

Hypervolume is used to measure the 'volume' in the objective space covered by the non-dominated solutions for minimization problems. The value is denoted as HV and is calculated as

$$HV = \text{volume}\left(\bigcup_{i=1}^{|ND|} v_i\right) \tag{14}$$

where $|ND|$ is the number of solutions in the obtained non-dominated set and v_i is the hypercube containing the origin and is bordered by hyperplanes passing through solution i in the objective space, with one hyperplane for each objective perpendicular to the objective's axis.

4. Results and analyses

4.1 Experimental background

This section provides a detailed description of the numerical experiments with different scales. The satellite set in our experiment is a Chinese GEO satellite in orbit with a payload that consists of a camera with visible light 50 m resolution and more than 400 km in width. The orbital elements are listed in Table 2.

Table 2 Satellite parameters

Parameter	Value
Height/km	36 000
Eccentricity	0
Inclination /(°)	40
Perigee /(°)	40
RAAN/(°)	190
Mean anomaly/(°)	0

In this paper, the experimental scenario is abstract, and all point targets are only scanned once. Based on the observation ability of the satellite and the mathematical model built in Section 4, we set $L = 7\ 000$ km and $r = 400$ km. Some assumptions are: (i) no deformation of single grid size; (ii) no consideration of cloud effect; (iii) each point target can be successfully identified by the satellite; (iv) satellites have sufficient electrical power and storage; and (v) in order to ensure the closure of the TSP results, each time after the completion of the observation task, the camera of satellite will return to the starting position.

The proposed multi-objective mission planning optimization method is verified by using PYTHON code running on a PC with an Intel Core i7 processor operating at 3.30 GHz with 4 GB RAM.

4.2 Point targets with a random distribution

4.2.1 Generation of test instances and parameter choices

The first experiment mainly focuses on point targets with random distribution, which is more general. The test instances are generated randomly and mainly include two parts. One is the coordinates of all point targets, which are randomly generated in the range of $[x_{\min}, x_{\max}]$ and $[y_{\min}, y_{\max}]$. The other one is the profit of each photo p_m, which is integer and generated in the interval of [1,5].

Based on the number of point targets and the number of photos, the case sizes can be divided into three levels: small scale, medium scale, and large scale. Table 3 gives the simulation parameters for different scenarios (N_{pop} is the number of individuals in each generation, N_{gen} is the generation of the NSGA-2 algorithm, p_c is the crossover probability, and p_m is the mutation probability).

Table 3 Simulation parameters for different scenarios

Scenario	Number of targets/m	Number of photos/n	N_{pop}	N_{gen}	p_c	p_m
1	25	10	150	200	0.9	0.1
2	50	20	150	200	0.9	0.1
3	75	40	150	200	0.9	0.1

In order to avoid the impact of randomness on the algorithmic results, 20 independent runs are performed and non-dominated solutions from each run are recorded.

4.2.2 Non-dominated set obtained

We obtain non-dominated sets for three different types of scale tasks after a 200 generation iteration and the Pareto frontier is shown. Fig. 11 is one group of Pareto frontiers of three different scenarios selected from the 20 independent runs of the algorithm.

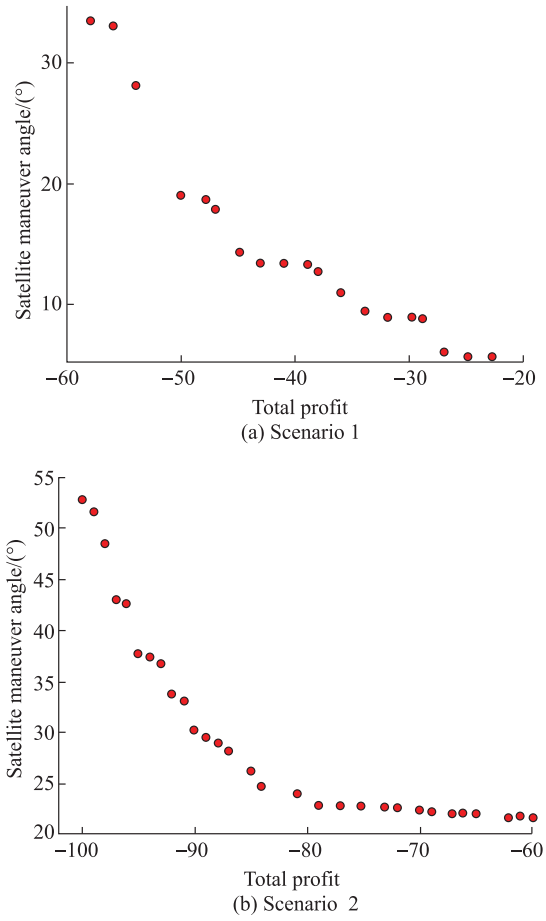

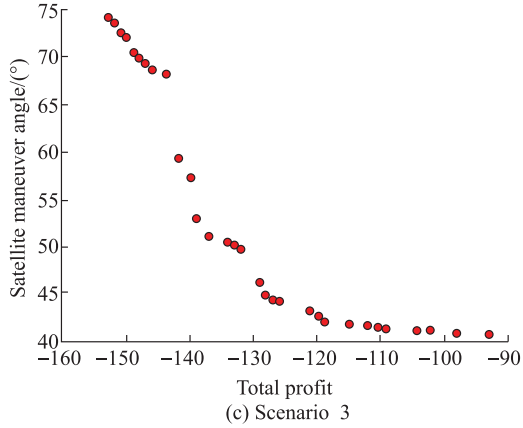

Fig. 11 One group of Pareto frontiers selected of three different scenarios

Decision makers can benefit from examining the trade-off between the objective function values of the encountered non-dominated sets. In all three different scale tasks, it can be observed that the two objectives are conflicted: if the expected profit is maximized, then the adjustment angle tends to increase.

In daily use of GEO satellites, this paper uses the medium-scale task as an example for further analysis. In Fig. 12, the non-dominated set can be roughly partitioned into two sets: 1 and 2. The solution in Set 1 has a low profit, and a linear approximation would have a slightly negative slope. The maneuver angle of this subset is stable in the interval [21.5, 24], while the profit varies between 60 and 81. This indicates that decision makers can significantly increase the expected profit at the expense of a slight increase in the maneuver angle. Set 2 shows that, from an expected profit of 86 onwards, if decision makers wish to further improve the profit, a large sacrifice is required with respect to the balance of the satellite attitude maneuver angle. A final decision depends on the preference regarding the objectives of the profit and the maneuver angle.

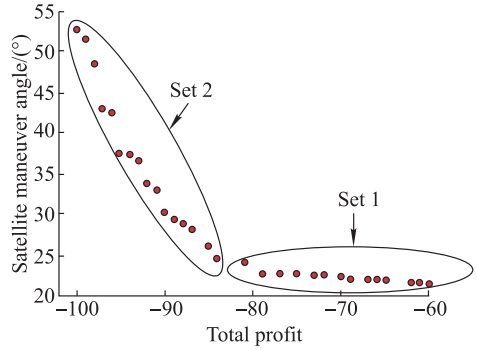

Fig. 12 Non-dominated solution obtained by HNSGA-II

4.2.3 Phenotype analysis

Fig. 13 is a visual representation of the point targets dis-

tribution and planning results. We show figures with max profit in generation 200 for small and medium scales. In the figure, dots represent point targets generated randomly and the number around each dot is the profit. The red square is the single view of the GEO satellite, where the number in the square is the order of each photo. From Fig. 13, it is clear that TSP optimization is performed on the sequence of photos. In the selected small and medium scale scenarios, the selection percentage of targets with revenue 5 are 89% and 90%, respectively. In order to analyze the profit gains of each photo, we obtain some statistics. In the small-scale case, the minimum profit of all photos is 5, the maximum profit is 13, and the average profit is 5.8. In the medium-scale case, the minimum profit of all photos is 1, the maximum profit is 10, and the average profit is 5. The visual representation directly shows that the algorithm can maximize the profit with the limitation of photos as possible.

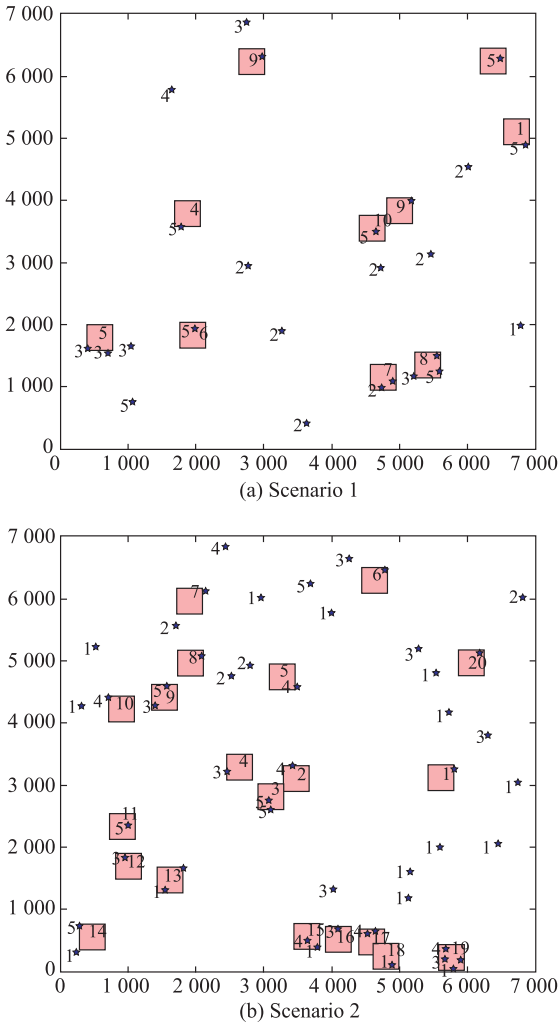

Fig. 13 Visual representation of the point targets distribution and planning results

4.2.4 Algorithm performance and comparison

A normalized treatment is carried out in the experiments. After selecting the reference point H (0, 300), we calculate the average hypervolume of each generation for three scenarios in 20 runs (depicted in Fig. 14).

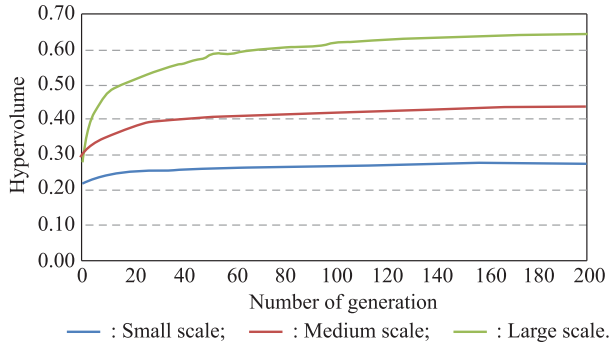

Fig. 14 Average hypervolume of each generation for three scenarios of HNSGA- II in 20 runs

In Fig. 14, as the number of generations increases, the hypervolume also increases, representing that a better Pareto solution is obtained. The proposed algorithm has good convergence in the three different scale scenarios; it converges in the first 20, 40 and 60 generations, respectively, after which the speed of convergence becomes slower. Overall, the algorithm remains stable in the 20 runs approaching the Pareto front.

As introduced above, the proposed algorithm is a variant of the NSGA-II algorithm. We compare the performance of the HNSGA-II algorithm with the simple one for three different scale cases, as depicted in Fig. 15 and Fig. 16.

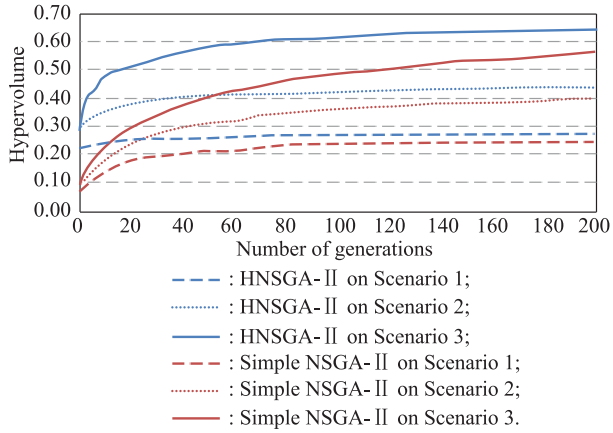

Fig. 15 Average hypervolume of each generation for three scenarios of two algorithms in 20 runs

Fig. 15 shows the iteration process for the two algorithms. Before 60 generations, the hypervolume of the simple NSGA-II algorithm is significantly smaller than

HNSGA-II, indicating that its performance in the initialization phase is much worse than the propsed algorithm, which affects the optimization efficiency. In order to verify whether the result after 200 generation of HNSGA-II is better than that of simple NSGA-II, we make a statistical analyses and depict it in Fig. 16.

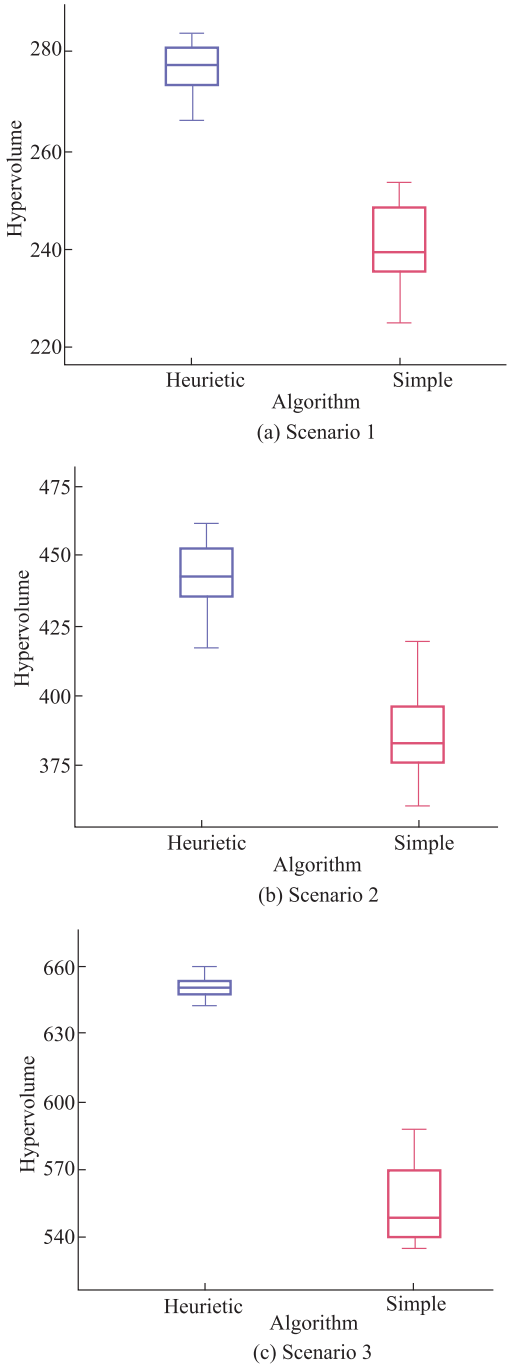

Fig. 16 Box plot of hypervolume for two algorithms performed on three scenarios

In Fig. 16, from left to right is the box plot of hypervolume for three scenarios. We have conducted statistical significance tests for these results for a significance level $\alpha = 0.05$ and we find that the performance of HNSGA-II is much better than the simple NSGA-II algorithm. And the difference becomes bigger as the task scale increases. It is proved that the heuristic principle make effects.

4.3 Further experiment

The above experiments focus on random distributions, which are more general. However, we are also faced with characteristic distributions. This further experiment uses one particular distribution of point targets and analyzes the performance of the proposed algorithm in order to examine model universality. This experiment could also determine which type of distribution can be better solved, thus giving guidance for the future use of GEO satellites.

A particular distribution is shown in Fig. 17, which can be described as multi-clustered targets. There are 50 point targets with four clusters distributed in the visual range of the GEO satellite, and there are also some scattered point targets.

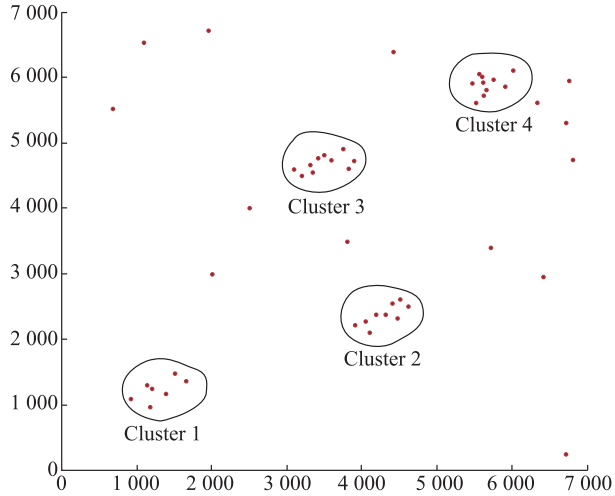

Fig. 17 Point targets with multi-clustered distribution

Experimental parameters are shown in Table 4, and 20 independent runs are performed.

Table 4 Experimental parameters of Scenario 4

Scenario	Number of targets/m	Number of photos/n	N_{pop}	N_{gen}	p_c	p_m
4	50	15	150	200	0.9	0.1

In Fig. 18, red dots are a selected Pareto Frontier of generation 200 in 20 runs, which indicates the process of the satellite taking photos. Note the zooming point around a profit of 130. This implies that the point targets of the four clusters are all observed, and decision makers can give up other scattered point targets if they do not want to sacrifice satellite maneuver angles. Compared with the Scenario 2

in Fig. 11, the multi-cluster distribution of point targets has bigger profit with fewer photos due to its distribution characteristics.

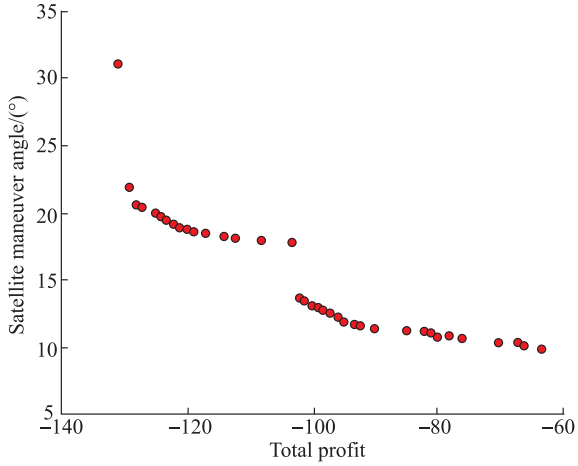

Fig. 18 A selected Pareto frontier of generation 200 for Scenario 4 in 20 runs

Fig. 19 depicts the change of hypervolume when performing the HNSGA-II algorithm on point targets with multi-clustered distribution in 20 runs. We can also find that the convergence of the improved algorithm is good when faced with this kind of distribution.

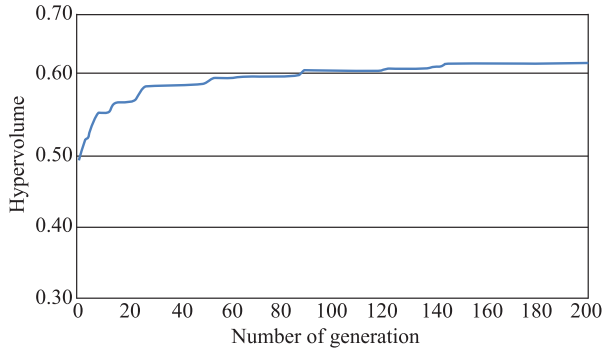

Fig. 19 Average hypervolume of each generation for Scenario 4 in 20 runs

From the results shown above, we can draw a conclusion that the proposed algorithm is very suitable for multi-clustered distribution, and this kind of phenomenon can give some application guidance to satellite control agency and users, that is, GEO satellite is very suitable for observing multi-clustered point targets in a large area.

5. Conclusions

In this paper, basic information and the general working pattern of GEO optical satellites are summarized. A target observation mission planning model for GEO satellites is proposed. After analyzing the requirements of users and satellite control agencies, two objectives are simultaneously considered: maximization of the profit and minimization of the satellite attitude maneuver angle. An NSGA-II based algorithm HNSGA-II algorithm is designed for solving this model, where we add a heuristic principle in the initialization phase, a mutation operator, and embeded TSP optimization.

In order to examine the proposed algorithm's performance, we calculate the hypervolume, and the improved algorithm shows good convergence. When performed on a random distribution of point targets, compared with the simple NSGA-II algorithm, the improved algorithm shows better performance in the initialization phase and it can obtain better Pareto frontier.

Different types of distributions are considered. With a multi-clustered distribution, we find that the proposed algorithm is very suitable, which could provide guidance on the further use of GEO satellites.

References

[1] B. N. Zhang. Survey on technical development of optical remote sensor on Chinese resource satellite. *Proc. of Chinese Space Science and Space Exploration Society of Professional Committee of Twenty-Sixth National Symposium on Space Exploration*, 2013: 327 – 333. (in Chinese)

[2] L. H. Guo, Z. Deng, J. S. Lao, et el. Preliminary research on development of foreign geo remote sensing satellites. *Spacecraft Recovery and Remote Sensing*, DOI: 10.3969/J.issn.1009-8518.2010.06.004. (in Chinese)

[3] R. Xavier. From Meteorology globe observation to high resolution permanent surveillance, 2007, IAC-070B1.2.06.

[4] D. Pawlak, R. Cantie. GEO-AFRICA: a dedicated african space observatory. *Proc. of the 60th International Astronautical Congress*, 2009, IAC-09-B1.2.3.

[5] J. C. Lin, L. W. Sun, F. S. Chen. Research on Geo-Oculus — a geostationary high resolution camera. *Infrared*, 2012, 33(5): 1 – 6. (in Chinese)

[6] W. Ma, J. Shi. Technical characteristics of "GF-4" satellite staring camera. *Space Flight Return and Remote Sensing*, 2016, 37(4): 26 – 31.

[7] S. W. Baek, S. M. Han, K. R. Cho, et al. Development of a scheduling algorithm and GUI for autonomous satellite missions. *Acta Astronautica*, 2011, 68(7): 1396 – 1402.

[8] H. S. Hebb. Artificial intelligence applications in aerospace. *St Johns Law Review*, 2011, 85(1): 218 – 220.

[9] P. Tangpattanakul, N. Jozefowiez, P. Lopez. A multi-objective local search heuristic for scheduling earth observations taken by an agile satellite. *European Journal of Operational Research*, 2015, 245(2): 542 – 554.

[10] D. Zhang, L. Guo, Q. Wang, et al. An improved single-orbit scheduling method for agile imaging satellite towards area target. *Geomatics & Information Science of Wuhan University*, 2014, 39(8): 901 – 905, 922. (in Chinese)

[11] S. Liu, Y. Chen, L. Xing, et al. Time-dependent autonomous task planning of agile imaging satellites. *Journal of Intelligent and Fuzzy Systems*, 2016, 31(3): 1365 – 1375.

[12] X. L. Liu, W. Jiang, Y. J. Li. Mutation particle swarm optimization for earth observation satellite mission planning. *Proc. of IEEE International Conference on Management Science and*

Engineering, 2013: 236 – 243.
[13] Y. He, Y. Wang, Y. Chen, et al. Auto mission planning system design for imaging satellites and its applications in environmental field. *Polish Maritime Research*, 2016, 23(s1): 59 – 70.
[14] A. Tarasyuk, I. Pereverzeva, E. Troubitsyna, et al. The formal derivation of mode logic for autonomous satellite flight formation. *Proc. of International Conference on Computer Safety, Reliability, and Security*, 2015, 9337: 29 – 43.
[15] E. M. Middleton, S. G. Ungar, D. J. Mandl, et al. The earth observing one (EO-1) satellite mission: over a decade in space. *IEEE Journal of Selected Topics in Applied Earth Observations & Remote Sensing*, 2013, 6(2): 243 – 256.
[16] N. A. Titus. Optimal station-change maneuver for geostationary satellites using constant low thrust. *Journal of Guidance Control & Dynamics*, 2015, 18(5): 1151 – 1155.
[17] Y. Zhou, Y. Yan, X. Huang, et al. Mission planning optimization for multiple geosynchronous satellites refueling. *Advances in Space Research*, 2015, 56(11): 2612 – 2625.
[18] D. K. Petraki, M. P. Anastasopoulos, T. Taleb, et al. Positioning in multibeam geostationary satellite networks. *Proc. of IEEE International Conference on Communications*, 2009, 42(2): 1 – 5.
[19] H. Akimotom, Y. Kasai, K. Kita, et al. Geostationary atmospheric observation satellite plan in Japan (Invited). *Proc. of AGU Fall Meeting*, 2009: 1 – 5.
[20] U. Finke, O. Kreyer. Detect and locate lightning events from geostationary satellite observations, 2002, EUM/CO/02/1016/SAT.
[21] S. B. Chen, Y. Yang. Study of the cloud effect on lightning detection by geostationary satellite. *Chinese Journal of Geophysics*, 2012, 55(3): 797 – 803.
[22] J. Orphal, G. Bergametti, B. Beghin, et al. Monitoring tropospheric pollution using infrared spectroscopy from geostationary orbit. *Comptes Rendus Physique*, 2005, 6(8): 888 – 896.
[23] X. J. Li, J. H. Zhou, L. Liu, et al. Research on technique of single-satellite orbit determination for geo satellite of partial subsatellite point. *Lecture Notes in Electrical Engineering*, 2013: 163 – 172.
[24] J. Xiong, X. Tan, K. Yang, et al. A hybrid multiobjective evolutionary approach for flexible job-shop scheduling problems. *Mathematical Problems in Engineering*, 2012: 857 – 868.
[25] J. Xiong, Y. W. Chen, K. Yang, et al. A hybrid multiobjective genetic algorithm for robust resource-constrained project scheduling with stochastic durations. *Mathematical Problems in Engineering*, 2012: 131 – 152.
[26] K. Deb, J. Sundar. Reference point based multi-objective optimization using evolutionary algorithms. *Proc. of Conference on Genetic and Evolutionary Computation*, 2006, 2: 635 – 642.
[27] C. A. C. Coello, G. B. Lamont, D. A. V. Veldhuizen. *Evolutionary algorithms for solving multi-objective problems*. New York: Springer, 2007.
[28] K. Deb, A. Pratap, S. Agarwal, et al. A fast and elitist multiobjective genetic algorithm: NSGA-II. *IEEE Trans. on Evolutionary Computation*, 2002, 6(2): 182 – 197.
[29] C. Q. Zhang, J. G. Zheng, J. Qian. Comparison of coding schemes for genetic algorithms. *Application Research of Computers*, 2011, 28(3): 819 – 822.
[30] E. Zitzler, L. Thiele. Multiobjective evolutionary algorithms: a comparative case study and the strength pareto approach. *IEEE Trans. on Evolutionary Computation*, 2000, 3(4): 257 – 271.

Biographies

Jiting Li was born in 1993. He received his B.S. degree in management engineering, from National University of Defense Technology, Changsha, China. He is currently working towards his M.S. and Ph.D. degrees in system optimization at National University of Defense Technology, Changsha, China. His research is mainly about satellite mission planning and scheduling.
E-mail: lijiting@nudt.edu.cn

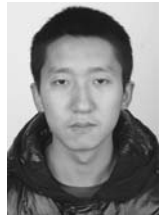

Sheng Zhang was born in 1993. He is currently working towards his M.S. and Ph.D. degrees in National University of Defense Technology. So far he has published several research papers. His current research interests include optimization algorithm, machine learning, and data mining.
E-mail: zhangsheng@nudt.edu.cn

Xiaolu Liu is a lecturer from National University of Defense Technology. She received her B.S. degree and Ph.D. degree both from National University of Defense Technology in 2006 and 2011, respectively. Her research interests include scheduling of imaging satellites and optimization of earth observation satellite system.
E-mail: lxl_sunny_nudt@live.cn

Renjie He was born in 1974. He is a professor at the School of Information System and Management, National University of Defense Technology. His main research interest is technology of system optimization and decision analysis.
E-mail: renjiehe@nudt.edu.cn